JOURNAL OF APPLIED ELECTROCHEMISTRY 20 (1990) 885–892

Mass transfer in a laminar-flow parallel plate electrolytic cell with simultaneous development of velocity and concentration boundary layers

JIAN QI, R. F. SAVINELL*

Department of Chemical Engineering, Case Western Reserve University, Cleveland, Ohio 44106, USA

Received 14 August 1989; revised 7 February 1990

Ionic mass transfer in a parallel plate electrochemical cell having a flow entrance representative of practical industrial cells has been studied under laminar flow condition using the ferri- and ferrocyanide redox couple. The working electrode was segmented so that local mass transfer coefficient could be measured. The mass transfer coefficients measured for the entrance region of the cell, which is defined as the region where both hydrodynamic and concentration boundary layers are developing simultaneously, are correlated and compared with results from other studies. For the electrode section beyond the entrance region, where the flow is fully developed but the concentration boundary layer continues to grow, a correction term is added to the electrode dimension parameter in the Graetz number. In this way the Leveque equation can still be used to correlate the local mass transfer coefficient. The value of the correction term is calculated by matching the downstream mass transfer boundary layer thickness to that of a Leveque-type cell. This scheme improves substantially the convergence of the experimental data correlation and results in good agreement with the Leveque equation.

Nomenclature

B width of electrode (cm)
d_e equivalent diameter of cell, $2SB/(B + S)$ (cm)
D diffusion coefficient of ferricyanide ($cm^2\,s^{-1}$)
k_y local mass transfer coefficient at y ($cm\,s^{-1}$)
k_{L_e} local mass transfer coefficient at $y = L_e$ ($cm\,s^{-1}$)
$k_{y'}$ local mass transfer coefficient at $y = y'$ ($cm\,s^{-1}$)
k_{av} average mass transfer coefficient over electrode length L ($cm\,s^{-1}$)
l concentration boundary layer thickness in developing flow cell (cm)
l' concentration boundary layer thickness in Leveque-type cell (cm)
L electrode length (cm)
L_e hydrodynamic entrance length (cm)
S gap distance between electrode and opposite wall (cm)
U_{av} average electrolyte flow velocity ($cm\,s^{-1}$)
x_0 the length of leading inert section of electrode (cm)
$X = x_0 + L$ (cm)
y distance from beginning of active mass transfer section in the channel (cm)
y' distance equivalent to L_e in Leveque-type of cell (cm)
y_i distance from mass transfer starting point in the channel to the upstream edge of electrode segment i (cm)
y_{i+1} distance from mass transfer starting point in the channel to the downstream edge of electrode segment i (cm)
Y modified electrode coordinate (cm)
$Y_i = y_i - L_e + y'$ (cm)
$Y_{i+1} = y_{i+1} - L_e + y'$ (cm)
γ respect ratio, S/B
Γ ionic strength
ρ density of electrolyte ($g\,cm^{-3}$)
μ viscosity of electrolyte (poise)

Dimensionless groups
Gz Graetz number, $Sc\,Re\,d_e/y$
Re Reynolds number, $\rho U_{av} d_e/\mu$
Re_L Reynolds number, $\rho U_{av} L/\mu$
Re_X Reynolds number, $\rho U_{av} X/\mu$
Sc Schmidt number, $\mu/\rho D$
Sh Sherwood number, $k_y d_e/D$
Sh_L Sherwood number, $k_{av} L/D$
Sh_X Sherwood number, $k_{av} X/D$

Subscripts
av average
e equivalent or entrance
y electrode length coordinate

* To whom correspondence should be addressed.

0021-891X/90 $03.00 + .12

1. Introduction

Electrochemical cells with forced convection offer many advantages and find wide applications in the electrochemical industry. Frequently, the performance of an electrochemical process is limited by mass transfer of reactant species or deteriorated by the presence of reaction products. A cell with high flow velocities can greatly increase mass transfer coefficient and facilitate the subsequent removal of reaction products, as well as assist thermal management and homogenize electrolyte. From a practical point of view, a parallel plate cell, which consists of two electrodes placed on the opposite sides of a rectangular duct, is an often favoured geometry.

There are a number of publications dealing with the mass transfer in a parallel plate cell with flowing electrolyte [1–5]. A popular approach to such a problem is to disentangle the mass transfer from the fluid flow complications. Experimentally, an inert zone is commonly added between the entrance of a cell channel and the electrode to assure a fully developed flow [1, 3, 4]. In this way, the hydrodynamic condition is constant along the electrode and, in laminar flow, a parabolic velocity profile results. For mass transfer under fully developed laminar flow, the Leveque–Graetz treatment leads to the Leveque equation and provides an excellent theoretical basis for predicting and correlating the mass transfer coefficient [6, 7]; and most experimental results show fairly good agreement with the Leveque-type correlation.

However, practical cells often do not have an entrance length to assure a fully developed flow. In many cases, developing flow is desirable since it will give rise to enhanced mass transfer. The mass transfer problem under developing flow condition appears to be more complex, but it can still be theoretically treated for laminar flow using the boundary layer theory, which predicts the thickness of a developing velocity boundary layer. The mass transfer boundary layer thickness is then estimated by multiplying the velocity boundary layer by $Sc^{-1/3}$ [8].

In contrast to the experimental information available for systems with fully developed laminar flow, relatively little work has been reported for cells involving developing flow. Although the earlier work by Wranglen and Nilsson [1] indicated that the mass transfer coefficient in developing flow is proportional to $U_{av}^{1/2}$, a theoretical prediction from the boundary layer theory, different proportionality coefficients were obtained. The correlation obtained experimentally by Pickett and Ong [5] took into account the hydrodynamic entrance length but seems only applicable to the situation where the entire electrode is nearly fully occupied by developing flow. In addition, the measurements and use of average mass transfer coefficient of an entire electrode in their studies tend to obscure the difference between the developing and fully developed conditions.

This study is stimulated by the need to develop a general method for correlating the local mass transfer coefficient for a parallel plate cell encompassing both laminar flow developing and fully developed regions. Apparently, the mass transfer coefficient in the fully developed flow region differs from the prediction of Leveque correlation, due to influence of entrance mass transfer on the concentration boundary layer development. A scheme for correlating mass transfer in laminar flow is devised in this work to take into account this influence. Experimental data from a practical electrolyzer design are used to develop a correlation for the entrance region and then to demonstrate this correlation scheme for the fully developed flow region. Another motivation for this study is a rather practical one, i.e., to provide experimental data for the theoretical modelling of the performance of an aluminium/air battery system [9, 10].

2. Experimental details

Ferricyanide reduction was employed for limiting current measurements in a simulated electrolyzer. The experimental electrolyzer design was adapted from an aluminium/air battery design [9, 11] and represents a typical arrangement where fluid enters a channel electrolyzer without adequate space for flow development to take place. The experimental cell simulates the gap and length but only represents one of many parallel channels in an actual cell. A sketch of the working electrode compartment assembly is shown in Fig. 1, which consisted of a rubber spacer and two plexiglas plates, with a segmented nickel electrode embedded in one of them. Mylar film was used to separate the nickel segments. By using plexiglas, the hydrogen evolution can be readily seen and the presence of air bubbles clinging to the electrode during the experiments can be checked. There were three holes of about 3 mm diameter each at the inlet of the working electrode compartment to serve as a flow distributor. A capillary hole was placed near the outlet edge as the reference electrode port. The two configurations of the segmented electrode used are shown in Fig. 2.

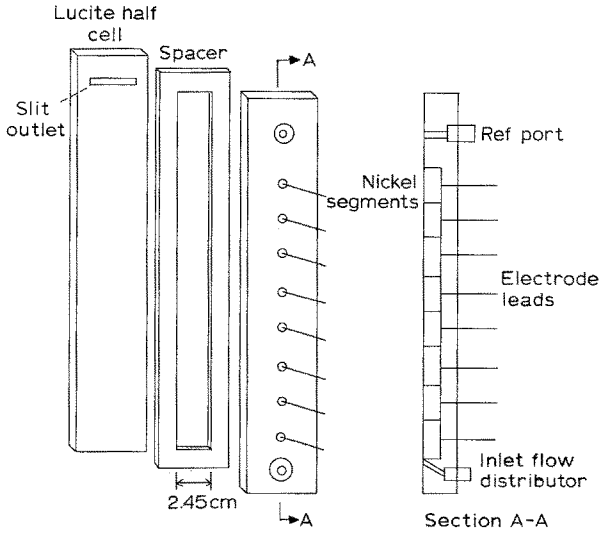

Fig. 1. Assembly of working electrode compartment.

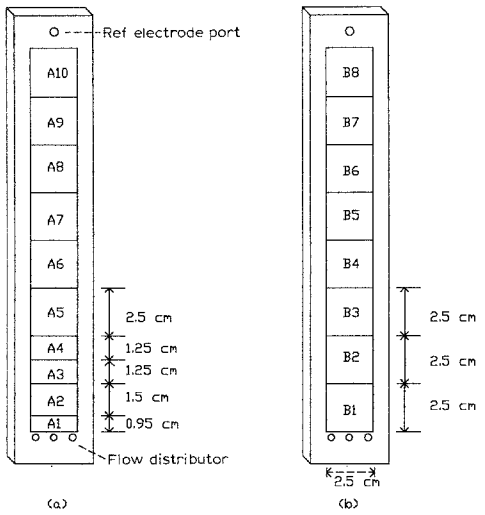

Fig. 2. Two configurations of segmented electrode.

A schematic diagram of the electrolyte flow system is shown in Fig. 3, where the counter electrode, whose compartment was located downstream of the working electrode, was constructed of a nickel mesh. All piping and pumping was made of PVC or other corrosion resisting materials. Constant temperature was maintained in the reservoir with a cartridge heater and a thermocouple temperature sensor, both placed inside nickel sheaths. The temperature was set such that the working electrode compartment was at the desired temperature.

The reference electrode was Hg/HgO in KOH solution. Fresh electrolyte was prepared before each experiment by dissolving equimolar potassium ferricyanide and ferrocyanide in KOH solution. All chemicals used were reagent grade. Since ferricyanide can decompose slowly in base to form cyanide ions, and ferrocyanide when exposed to light also slowly hydrolyzes to produce cyanide, the concentration of the reactant gradually decreased. The cyanide product from these reactions also poisons the nickel electrode surface. Therefore the entire system was light shielded, except for the working electrode compartment, to minimize the spontaneous degradation of solutions. Furthermore, nitrogen gas was bubbled through the system reservoir to deaerate the electrolyte so that decrease in ferricyanide concentration was less than 2% in all the experiments.

During each experiment, the actual ferricyanide concentration was analyzed iodimetrically. The titration procedure described in [12] was adopted with some modifications: Prior to the titration given in [12], the sample solution was neutralized with concentrated sulphuric acid after precipitating ferrocyanide with zinc sulphate. The method was tested to give error less than 4%, based on more than ten titrations of standard potassium ferricyanide solution in 5 M KOH, which was prepared according to [13].

The electrode was polished before experiments with alumina powder, washed with distilled water and ultrasonically cleaned. After each increment of applied potential, five to ten minutes were allowed for steady state current readings. Current passing each electrode segment was measured simultaneously with an eight-channel current follower, until all the segments reached limiting current.

From the measured limiting currents on each segment of the electrode, the average mass transfer coefficient and the Sherwood number on that segment were calculated. The density and viscosity of aqueous potassium hydroxide solution at different temperatures and concentrations can be found from [14] and the values for the solutions in this study are listed in Table 1.

Electrolyte temperature was varied from 40 to 60°C and potassium hydroxide concentration from 2 M to 5 M. Both electrode configurations shown in Fig. 1 were used to measure local limiting current at various flow velocities.

In order to compute the Sherwood number, the diffusion coefficient must be known. There have been several studies on the diffusion coefficient of ferricyanide ions in potassium hydroxide solution [15–17], among which Gordon, *et al.* [16] correlated their data in the form of the Stokes–Einstein parameter, $D\mu/T$, as a function of ionic strength of KOH solution, Γ, the results being:

$$\mu D/T = (2.344 + 0.014\Gamma \pm 0.05) \times 10^{-10}\ \text{dyne K}^{-1} \quad (1)$$

The measurements made by Arvia *et al.* [17] at 24 to 50°C and KOH concentrations of 0.5 to 2 M led to the following equation:

$$\mu D/T = (2.78 \pm 0.18) \times 10^{-10}\ \text{dyne K}^{-1} \quad (2)$$

Since both equations seem reliable and the discrepancy between them is small when the ionic strength of

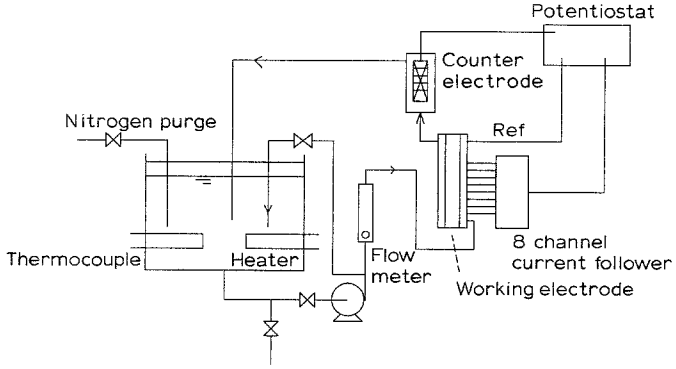

Fig. 3. Diagram of experimental setup.

Table 1. Values of density and viscosity of KOH solution and diffusion coefficient of ferricyanide

KOH conc. (M)	*Temp.* (°C)	ρ ($g\,cm^{-3}$)	μ (*cp*)	D ($cm^2\,s^{-1}$)
2	40	1.08	0.82	1.0×10^{-5}
2	60	1.07	0.58	1.5×10^{-5}
5	60	1.19	0.84	1.0×10^{-5}

5 M KOH solution is considered in Equation 1, the average of these two equations is used in this study to evaluate ferricyanide diffusion coefficient:

$$\mu D/T = 2.6 \times 10^{-10}\ \text{dyne K}^{-1} \qquad (3)$$

This equation also is used to evaluate D in 2 M KOH solution, since the effect of ionic strength shown in Equation 1 is not very significant. The calculated diffusion coefficients using Equation 3 are given in Table 1.

3. Results and discussions

The mass transfer coefficients measured from each segment using electrode configuration (a) shown in Fig. 2 are listed in Table 2, while those obtained using configuration (b) are in Table 3.

3.1. *Leveque correlation*

For a parallel plate cell in which mass transfer commences after flow becomes fully developed, a Leveque-type equation should apply [18, 19]:

$$Sh = 0.978(Re\,Sc\,d_e/y)^{\frac{1}{3}}\left(\frac{2}{\gamma+1}\right)^{\frac{1}{3}} \qquad (4)$$

in which Sh is the Sherwood number defined as $k_y d_e/D$, where k_y is the local mass transfer coefficient at distance, y, downstream away from the mass transfer starting point, and d_e, the equivalent diameter, is equal to $2BS/(B+S)$; Re is the Reynolds number based on the equivalent diameter, viz., $Re = U_{av} d_e/\nu$; γ is called the respect ratio, defined as S/B, where B and S are the width and gap distance of the cell, respectively. The dimensionless group, $Re\,Sc\,d_e/y$, is known as the Graetz number, denoted by Gz. Note that the Leveque equation should be applied only for the region $y < 0.005\,Re\,Sc\,d_e$ (viz., $Gz > 200$) [20]. But this condition is generally satisfied in industrial cells.

Table 2. Mass transfer coefficients measured at each segment for cell configuration (a) under different average flow velocities

Run	U_{av} ($cm\,s^{-1}$)	*Mass transfer coefficient* $k \times 10^3$ ($cm\,s^{-1}$)							
		A1	*A2*	*A3*	*A4*	*A5*	*A6*	*A7*	*A8*
1	6.6	O	O	O	2.07	1.08	0.87	0.78	0.69
2	13.2	O	O	O	2.81	1.44	1.17	1.08	0.92
3	13.2	O	O	2.79	1.80	1.26	1.09	1.03	0.92
4	13.2	O	3.30	1.92	1.59	1.14	1.05	0.99	0.85
5	17.3	O	O	O	3.07	1.44	1.24	1.14	0.98
6	20.0	O	O	O	3.21	1.63	1.31	1.17	1.00
7	6.6	3.20	1.72	1.19	1.12	0.86	0.79	0.74	0.73
8	13.2	4.60	2.37	1.77	1.46	1.08	1.00	0.93	0.85
9	17.3	5.04	2.67	2.14	1.73	1.17	1.04	0.97	0.89

Unactivated (open circuit) segments are indicated by O.
5 M KOH; 60°C; $[K_3Fe(CN)_6] = 0.0076 - 0.0072$ M;
Equimolar ferri- and ferro-cyanide; $S = 0.165$ cm; $B = 2.45$ cm.

As can be seen from Table 2, runs 1–6 were performed with mass transfer commencing after passing several unactivated segments. The unactivated segments preceding the mass transfer allow a parabolic flow to develop and hence serve as the hydrodynamic entrance region. Since the measured mass transfer coefficient is the average value of each electrode segment, the value of y representing the segment needs to be determined in order to apply Equation 4 properly. According to Equation 4, we have:

$$(Re\,Sc\,d_e/y)^{\frac{1}{3}} = \frac{1}{y_{i+1}-y_i}\int_{y_i}^{y_{i+1}} (Re\,Sc\,d_e/y)^{\frac{1}{3}}\,dy \qquad (5)$$

where y_i and y_{i+1} are the distances of upstream and downsteam edges of the segment i to the mass transfer commencing point, respectively. Solving Equation 5, we obtain:

$$y = \left[\frac{2(y_{i+1}-y_i)}{3}\right]^3 (y_{i+1}^{\frac{3}{2}} - y_i^{\frac{3}{2}})^{-3} \qquad (6)$$

Table 3. Mass transfer coefficients measured at each segment of cell configuration (b) at various conditions

Run	*Temp.* (°C)	*KOH* (M)	U_{av} ($cm\,s^{-1}$)	*Mass transfer coefficient* $k \times 10^3$ ($cm\,s^{-1}$)							
				B1	*B2*	*B3*	*B4*	*B5*	*B6*	*B7*	*B8*
10	40	2	5.5	1.60	0.97	0.76	0.67	0.65	0.58	0.56	0.56
11	40	2	9.1	2.00	1.23	0.94	0.82	0.78	0.71	–	–
12	60	2	2.0	1.08	0.77	0.64	0.60	0.53	0.52	0.51	0.48
13	60	2	5.5	2.36	1.16	0.93	0.84	0.82	0.75	0.73	0.72
14	60	2	9.0	3.10	1.64	1.20	1.10	1.05	–	–	–
15	60	5	5.0	1.84	0.93	0.74	0.69	0.63	0.59	0.58	0.53
16	60	5	5.0	1.90	0.95	0.77	0.69	0.65	0.61	0.59	0.55
17	60	5	10.0	2.39	1.19	0.94	0.85	0.79	0.73	0.72	0.69
18	60	5	16.0	3.10	1.48	1.10	0.98	0.89	0.84	0.82	0.80

$[K_3Fe(CN_6] = 0.0076 - 0.0117$ M; Equimolar Ferri- and Ferrocyanide, $S = 0.2$ cm; $B = 2.45$ cm.

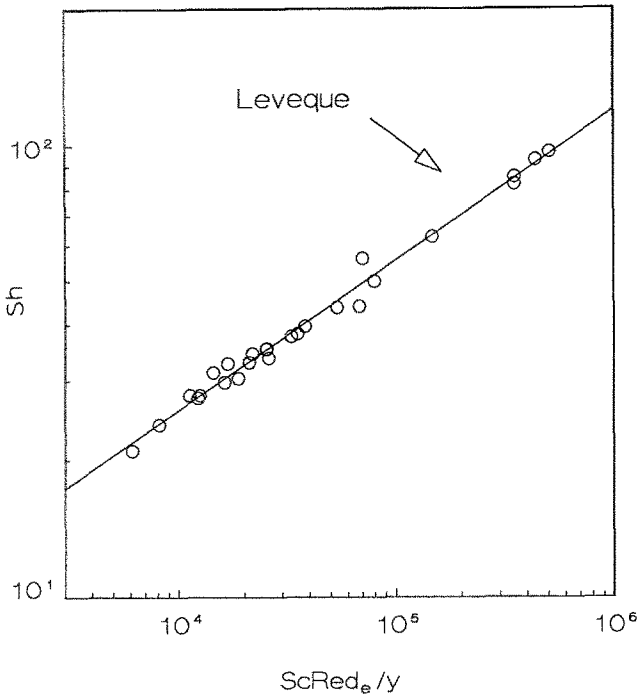

Fig. 4. Comparison of experimental data with the Leveque equation when there is a hydrodynamic entrance region present.

This equation was used for calculating the Graetz number, $Sc\,Re\,d_e/y$, for the experimental segments. The Sherwood number calculated from the mass transfer coefficients obtained from each segment in runs 1–3 and 5–6 is then plotted against the Graetz number in Fig. 4, where very good agreement with the Leveque equation is exhibited. However, it is worth noting that when data from run 4 are used the points from the first several segments tend to be much larger than Leveque prediction. In Fig. 5, the data from run 4 are compared with those from runs 2 and 3, which were at the same flow condition but with different unactivated entrance length. Apparently, the segment A2 is still in the flow developing region under this flow condition and thereby gives the mass transfer coefficient greater than the Leveque prediction. Furthermore, the mass transfer in the segments A3 and A4 in run 4 seems to be influenced by segment A2 and also tends to be greater, although the excellent agreement shown in Fig. 4 for runs 2 and 3 indicates that the flow appears to be fully developed when reaching segments A3 and A4.

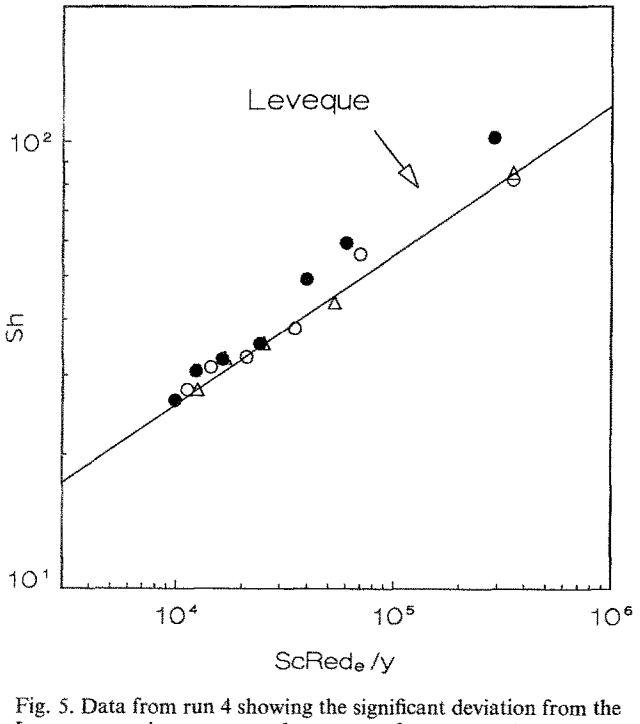

Fig. 5. Data from run 4 showing the significant deviation from the Leveque equation. △ = run 2; ○ = run 3; ● = run 4.

Another way to illustrate this is to estimate the hydrodynamic entrance length. The hydrodynamic entrance length is the distance downstream from the cell entrance needed for achieving fully developed flow. For laminar flow in a rectangular duct, there exist several equations to estimate this distance [18, 21, 22]. For the cell geometry in this study with a uniform entry velocity, the equation given in [22] should be appropriate [18]:

$$L_e = 0.01(10^{2.85y})d_e\,Re \tag{7}$$

Using the dimension given in Fig. 2 for cell configuration (a) and the Reynolds number calculated for run 4 ($Re = 578$), Equation 7 gives

$$L_e = 2.79\,\text{cm} \tag{8}$$

This value may not be exactly accurate due to the complication of the inlet stream distributor. (Equation 8 is probably an underestimate since the flow distributor tends to give a hydrodynamic entrance length longer than a uniform flow entry.) But it does indicate that the first two segments lie in the hydrodynamic entrance region and should have mass transfer values greater than the Leveque prediction.

In fact, significant scattering of data is observed if the Leveque equation is directly used to treat the data from runs 7 to 18, even for those segments under flow developed region. Note that there was no unactivated segment in these runs.

3.2. *Mass transfer in flow developing region*

It has been shown that flow in the parallel cell can be divided into two regions, flow developing region ($y < L_e$) and fully flow developed flow region ($y > L_e$). For the flow developing region, whose length can be estimated from Equation 7, the data obtained from the first several segments can be used to obtain a correlation. Based on Equation 7 and the results indicated in Fig. 4, we assume that segments A1 and A2 in run 7, segments A1, A2, and A3 in run 8, segments A1, A2, A3, and A4 in run 9, and segment B1 in runs 10 to 11 and 13 to 18 are in the flow developing region. (In run 12, only a very small portion of segment B1 could be considered to lie in the developing flow region due to the small Reynolds number.) Using the data of those segments, we obtain Fig. 6, where the straight line represents the equation:

$$Sh_L = Re_L^{\frac{1}{2}} Sc^{\frac{1}{3}} (d_e/L)^{-0.07} \tag{9}$$

Here the Sherwood and Reynolds numbers are defined

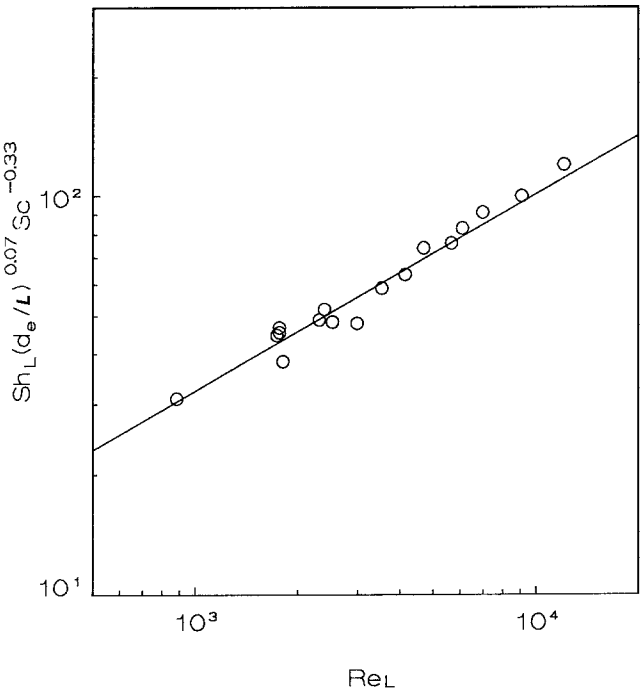

Fig. 6. Mass transfer correlation for flow developing region.

in terms of the electrode length, L, viz., $Sh_L = k_{av}L/D$ and $Re_L = U_{av}L/\nu$, where k_{av} represents the average mass transfer coefficient over the electrode length $L(L < L_e)$. Note that Equation 9 is very similar to that given in [18] at $x_0 = 0$, which is

$$Sh_X = 0.96Re_X^{\frac{1}{2}}Sc^{\frac{1}{3}}\frac{[1-(x_0/X)^{\frac{3}{4}}]^{\frac{2}{3}}}{1-(x_0/X)}(d_e/L)^{-0.05} \tag{10}$$

where $Sh_X = k_{av}X/D$; $Re_X = U_{av}X/\nu$; and $X = x_0 + L$; where x_0 is the distance from the entrance to the activated electrode. The flow distributor used in this study might contribute to the small discrepancy between Equations 9 and 10.

3.3. *Correlation for region of fully developed flow*

As mentioned earlier, the simultaneous development of the velocity and concentration boundary layers in the flow developing region may cause the mass transfer to differ from the Leveque prediction in the flow developed region of the developing flow cell in this study. To obtain a more accurate correlation, some modifications have to be devised to account for this difference.

Let us first analyze the entrance region of the developing flow cell. As shown in Fig. 7a, the velocity and concentration boundary layers are developing until reaching $y = L_e$. In the region $y > L_e$, the concentration boundary layer continues to grow while the velocity maintains parabolic profile. Because Equation 9 should apply in the region $y \leqslant L_e$, rearranging it yields:

$$k_{av}d_e/D = Re^{\frac{1}{2}}Sc^{\frac{1}{3}}(d_e/L)^{0.43} \tag{11}$$

Since the relationship between the average and local mass transfer coefficients is:

$$k_{av} = \frac{1}{L}\int_0^L k_y\,dy \tag{12}$$

we obtain the local mass transfer coefficient at position y:

$$k_y = \left(\frac{\partial(k_{av}L)}{\partial L}\right)_{L=y} \tag{13}$$

For Equation 11, this gives:

$$Sh = 0.57\,Re^{\frac{1}{2}}Sc^{\frac{1}{3}}(d_e/y)^{0.43} \tag{14}$$

Therefore, the local mass transfer coefficient, k_{L_e}, at the point where the flow just becomes fully developed is:

$$k_{L_e}d_e/D = 0.57\,Re^{\frac{1}{2}}Sc^{\frac{1}{3}}(d_e/L_e)^{0.43} \tag{15}$$

Figure 7b illustrates the cell to which the Leveque-type correlation applies. At a distance downstream from the entrance of a Leveque-type cell, the mass transfer boundary layer has the same thickness as that

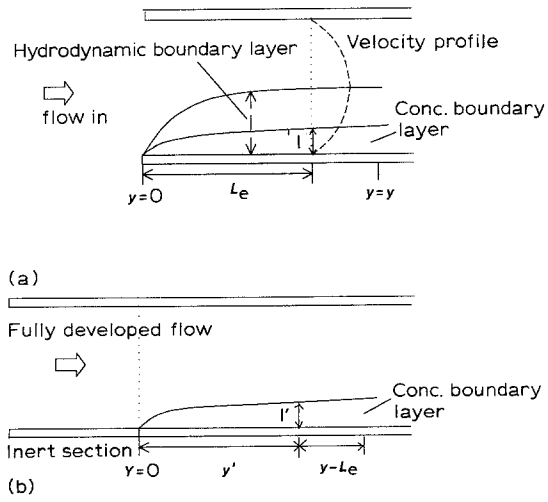

Fig. 7. (a) Entrance region of developing flow cell; (b) Leveque-type cell.

at L_e in the developing flow cell, or $l = l'$, as shown in Figs 7a and b. This distance, y', can be computed by equating $k_{y'}$ to k_{L_e} in Equations 4 and 15:

$$y' = 5.05\,Re^{-\frac{1}{2}} d_e^{-0.29} L_e^{1.29} \left(\frac{2}{\gamma + 1}\right) \quad (16)$$

Hence, the flow and mass transfer characteristics in the region $y \geqslant L_e$ of the developing flow cell (Fig. 7a) should be equivalent to that in $y \geqslant y'$ for the Leveque type cell. It then follows that the Leveque-type equation, or Equation 4, should be applicable to the flow region $y \geqslant L_e$ in the flow developing cell if we use

$$Y = y - L_e + y' \quad (17)$$

to replace y in the correlation, viz,

$$Sh = 0.978\,(Re\,Sc\,d_e/Y)^{\frac{1}{3}} \left(\frac{2}{\gamma + 1}\right)^{\frac{1}{3}} \quad (18)$$

Similarly, to use the experimental data of each electrode segment, a relation similar to Equation 6 should be used:

$$Y = \left[\frac{2(y_{i+1} - y_i)}{3}\right]^3 (Y_{i+1}^{\frac{3}{2}} - Y_i^{\frac{3}{2}})^{-3} \quad (19)$$

where $Y_i = y_i - L_e + y'$ and L_e and y' are calculated from Equations 7 and 16.

Substituting Equation 7 into Equations 16 and 17 and rearranging give

$$y' = 0.0133\,(10^{3.68\gamma}) d_e Re^{0.79} \left(\frac{2}{\gamma + 1}\right) \quad (20)$$

and

$$Y = y - 0.01\,(10^{2.85\gamma}) d_e Re + 0.0133\,(10^{3.68\gamma}) d_e Re^{0.79} \left(\frac{2}{\gamma + 1}\right) \quad (21)$$

This expression indicates that the correction term, $y' - L_e$, is a function of the respect ratio, γ, the equivalent diameter, d_e, and the Reynolds number, Re. It can be seen that at a certain critical value (or at zero) of Reynolds number, the term $y' - L_e$ becomes negligible and the mass transfer correlation will exactly follow the Leveque equation. When the Reynolds number is above that critical value, $y' - L_e$ is negative and the Graetz number will be greater than that calculated without the correction term, and vise versa. Furthermore, the influence of the correction term becomes diminishingly small as y increases. In this manner, the deviation illustrated in Fig. 4 can be compensated.

For run 4, the term $[1 - (x_0/X)^{\frac{3}{4}}]^{\frac{4}{3}}/[1 - (x_0/X)]$ in Equation 10 is very close to unity ($\simeq 1.04$ for the second segment). Thus the scheme devised above should also apply. Consequently, the data obtained from segments A3 to A8 in run 4 as well as from runs 7 to 18 are plotted in Fig. 8, with exclusion of those segments that are in the flow developing region (or have been used for Fig. 6). The Leveque equation is also plotted as a straight line in that figure to show the comparison. As can be seen, good convergency of data to a straight line and agreement with the Leveque equation are obtained.

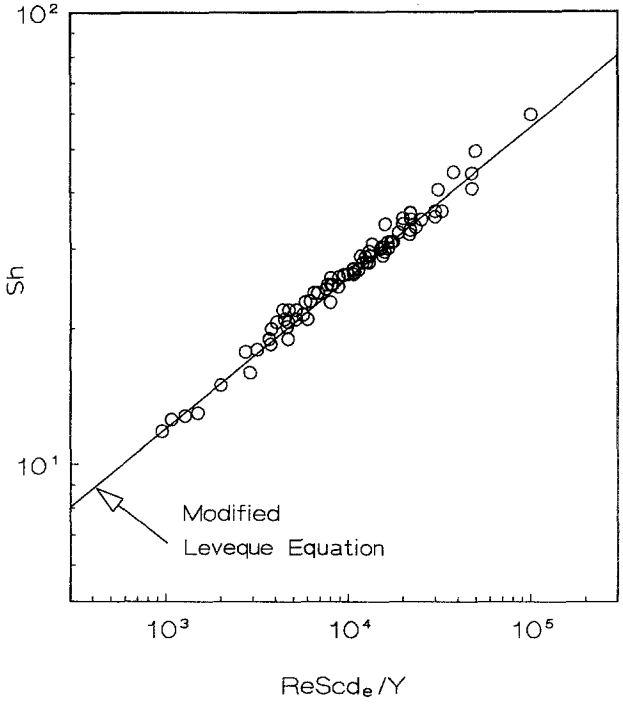

Fig. 8. Comparison of experimental data in developed flow region with the Leveque equation modified by the correction term.

4. Conclusions

The Leveque type of equation was derived with the assumption of a constant fully developed laminar flow as well as a homogeneous concentration boundary condition (i.e. a uniform surface concentration along the electrode), while Equation 10 should only be applicable to the situation where the hydrodynamic boundary layer is developing along the electrode. Neither is adequate in describing the mass transfer in a cell that encompasses both flow developing and fully developed regions. Therefore, the correlation of mass transfer should be considered separately for the two regions. Equation 9 is still applicable to the entrance region ($y < L_e$) of the flow cell; but for the fully developed flow region ($y > L_e$), the Leveque equation with modifications as given by Equations 17 should be used to yield a more convergent data representation. At $y = L_e$, both equations merge and give the same result. Although the prediction of the hydrodynamic entrance length by Equation 7 may not be very accurate due to specific details of distributor design in the experimental cell, introducing the correction term results in a substantial improvement in mass transfer data correlation. This is particularly effective at high Reynolds number and/or small y. Although this correlation scheme is demonstrated for laminar flow conditions, the methodology should be applicable to turbulent mass transfer problems.

Acknowledgement

This work has been funded by a subcontract (91087-RWF) from Eltech Systems Corporation, Cleveland,

Ohio for the development of aluminium/air battery for electric vehicle applications under U.S. DOE Sandia National Laboratory Contract No. 02-8199. The authors thank Dr. Eric Rudd and Doug Cole of Eltech Systems Corp. for their assistance in the experimental setup.

References

[1] G. Wranglen and O. Nilsson, *Electrochim. Acta* **7** (1962) 121.
[2] C. W. Tobias and R. G. Hickman, *Z. Phys. Chem.* (Leipzig), **229** (1965) 145.
[3] A. Palade de Iribarne, S. L. Marchiano and A. J. Arvia, *Electrochem. Acta* **15** (1970) 1827.
[4] D. J. Pickett and B. R. Stanmore, *J. Appl. Electrochem.* **2** (1972) 151.
[5] D. J. Pickett and K. L. Ong, *Electrochim. Acta* **19** (1974) 875.
[6] M. A. Leveque, *Ann. Mines* **13** (1928) 201, 305 and 381.
[7] L. Graetz, *Ann. Phys. Chem.* **25** (1885) 337.
[8] R. B. Bird, W. E. Stewart and E. N. Light, 'Transport Phenomena', John Wiley & Sons, New York (1960) p. 607.
[9] E. J. Rudd, in *Proceedings of the 33rd International Power Sources Symposium*, The Electrochemical Society, Pennington, NJ (1988).
[10] K.-Y. Chan and R. F. Savinell, Abstract No. 12, P17-18, 'Extended Abstract', **89-1**, Electrochem. Soc. Inc., Pennington, N.J.
[11] Personal Communication with E. J. Rudd of Eltech System Corp. referring to Progress Reports for the Department of Energy Contract SNLA 02–8199 (1988).
[12] A. Vogel, 'Textbook of Quantitative Inorganic Analysis', 4th ed., Longman Scientific & Technical, Harmondsworth (1978) p. 385.
[13] W. J. Blaedal and V. W. Meloche, 'Elementary Quantitative Analysis, Theory and Practice', 2nd ed., Harper & Row, New York (1963) p. 850.
[14] 'Caustic Potash Handbook', published by Diamond Shamrock Corp.
[15] C. S. Lin, E. B. Denton, H. S. Gaskill and G. L. Putnam, *Ind. Eng. Chem.* **43** (1951) 2137.
[16] S. L. Gordon, J. S. Newman and C. W. Tobias, *Ber. Bunsenges. Phys. Chem.* **70** (1966) 414.
[17] A. J. Arvia, S. L. Marchiano and J. J. Podesta, *Electrochim. Acta* **12** (1967) 259.
[18] D. J. Pickett, 'Electrochemical Reactor Design', Elsevier Scientific, New York (1977) pp. 133, 135, 140.
[19] J. R. Selman and C. W. Tobias, in 'Advances in Chemical Engineering', Vol. 10 (edited by T. B. Drew, G. R. Rokelet, J. W. Hooper, Jr. and T. Vermeulen), Academic Press, New York (1978).
[20] J. Newman, in 'Electroanalytical Chemistry', Vol. 6 (edited by A. J. Bard), Marcel Dekker, New York (1973).
[21] R. S. Brodkey, 'The Phenomena of Fluids Motion', Addison-Wesley (1967), p. 129.
[22] L. S. Han, *J. Appl. Mech.* **27** (1960) 403.